Published in final edited form as:
Science. 2008 July 4; 321(5885): 136–140. doi:10.1126/science.1159675.

The Spread of Ras Activity Triggered by Activation of a Single Dendritic Spine

Christopher D. Harvey[1,2,*], **Ryohei Yasuda**[2,3,*,+], **Haining Zhong**[1,2], and **Karel Svoboda**[1,2,+]

[1] Janelia Farm Research Campus, HHMI, Ashburn, VA 20147, USA

[2] Watson School of Biological Sciences, Cold Spring Harbor Laboratory, Cold Spring Harbor, NY 11724, USA

[3] Neurobiology Department, Duke University Medical Center, Durham, NC 27710, USA

Abstract

In neurons, individual dendritic spines isolate NMDA receptor-mediated Ca^{2+} accumulations from the dendrite and other spines. However, it is not known to what extent spines compartmentalize signaling events downstream of Ca^{2+} influx. We combined two-photon fluorescence lifetime imaging (FLIM) with two-photon glutamate uncaging to image the activity of the small GTPase Ras following NMDA receptor activation at individual spines. Induction of long-term potentiation (LTP) triggered robust Ca^{2+}-dependent Ras activation in single spines that decayed in approximately 5 minutes. Ras activity spread over approximately 10 micrometers of dendrite and invaded neighboring spines by diffusion. The spread of Ras-dependent signaling was necessary for the local regulation of the threshold for LTP induction. Thus Ca^{2+}-dependent synaptic signals can spread to couple multiple synapses on short stretches of dendrite.

Dendritic spines, small (< 1 μm^3) protrusions emanating from the dendritic shaft, are the sites of most excitatory synapses in the mammalian brain (1). Spines function as biochemical compartments (2,3) that isolate postsynaptic Ca^{2+} accumulations (4-6). Ca^{2+} influx through synaptic NMDA receptors (NMDA-Rs) activates a complex signaling network (7), including the small GTPase H-Ras (8-10), to induce long-term potentiation (LTP) of synaptic transmission (11,12). LTP is input specific (13), suggesting that important Ca^{2+}-dependent signals remain confined to single spines. In contrast, synapses interact through diffusible cytoplasmic factors (14-16). Which signals downstream of NMDA-R-dependent Ca^{2+} influx are restricted to individual spines? To begin to address this question, we imaged the dynamics of Ras activity during the induction of input-specific LTP.

We transfected pyramidal neurons in organotypic hippocampal slices with a fluorescence resonance energy transfer (FRET)-based indicator of Ras activation, FRas-F, consisting of H-Ras tagged with mEGFP and the Ras-binding domain (RBD, R59A mutation) of Raf tagged with two mRFPs (Fig. 1A) (17). Upon Ras activation, the affinity between Ras and RBD increases, leading to FRET between the donor and acceptor fluorophores (Fig. 1A) (17-19). FRas-F is rapidly reversible and reports the time course of endogenous Ras activation (17). We imaged FRET using two-photon fluorescence lifetime imaging (2pFLIM) (17,20,21). To quantify Ras activation, we computed the fraction of Ras molecules binding to RBD (binding fraction; Fig. 1B) (17,22).

+ To whom correspondence should be addressed. yasuda@neuro.duke.edu, svobodak@janelia.hhmi.org,.
*These authors contributed equally to this work.

To induce synapse-specific plasticity, we applied a train of two-photon glutamate uncaging pulses (30 pulses at 0.5 Hz) to a single spine in low (nominally 0 mM) extracellular Mg^{2+} (13,16). Each uncaging pulse produced $[Ca^{2+}]$ transients and NMDA-R-mediated currents (7.3 ± 0.6 pA, corresponding to the opening of ~ 5 NMDA-Rs), similar to those triggered by low frequency synaptic stimulation (Fig. S1) (6,22,23). Uncaging-evoked $[Ca^{2+}]$ accumulations were mostly restricted to the heads of the stimulated spines (Fig. S1A-E) (22). The uncaging train caused a sustained spine enlargement in the stimulated spine; neighboring spines less than 4 μm away did not change (Fig. 1C-E) (13,16). The increase in spine volume was proportional to an enhancement in postsynaptic sensitivity to glutamate, indicating that spine enlargement is a structural correlate of LTP (Fig. S2C) (13,16,24).

The uncaging train induced robust Ras activation in the stimulated spine (Fig. 1C, F-G), which peaked within one minute after the stimulus and returned to baseline levels within 15 minutes (τ_{decay} = 5.6 ± 0.5 min). Ras activation required Ca^{2+} influx through NMDA-Rs (Fig. 1H) (8-10). Ras activation also required the activity of multiple signaling factors; inhibitors of Calcium/calmodulin-dependent protein kinase II (CaMKII; 10 μM KN62), Phosphoinositide-3 kinase (PI3K; 20 μM LY294002), or Protein kinase C (PKC; 1 μM Gö6976) signaling reduced Ras activation (Figs. 1H, S3D) (11, 22, 25). The amplitudes of Ras activation and sustained spine enlargement were correlated (Fig. S4A). Expression of a dominant negative form of FRas-F (Ras S17N mutation) or inhibition of ERK activation (MEK blocker 10 μM U0126) reduced the magnitude of sustained spine enlargement (Fig. S4F) (22). Ras-ERK activation therefore was necessary for the persistent increase in spine volume, confirming the role of Ras signaling in synaptic plasticity (11). CaMKII activity, PKC signaling, and actin polymerization were also required for spine structural plasticity (Fig. S4F) (13, 22).

We next characterized the spatial profile of Ras activation (Figs. 1F-G, 2A-B). Following the plasticity-inducing stimulus, Ras activity spread over several micrometers in both directions along the parent dendrite and invaded nearby spines (length constant, $L \approx 11$ μm at 4 minutes; Fig. 2B), suggesting that Ras signaling is not synapse-specific.

Could the presence of the Ras sensor distort the spatial profile of Ras activity? The mean distance active Ras travels before it is inactivated, L, depends on the effective diffusion coefficient of Ras, D, and the time constant of Ras inactivation, $\tau_{inactivation}$ (22):

$$L \sim \sqrt{D\tau_{inactivation}} \qquad \text{Eq. 1}$$

FRas-F expression could increase D and $\tau_{inactivation}$ by saturating Ras scaffolds and Ras inactivators (GTPase activating proteins, GAPs), respectively. In addition, RBD competes with GAPs for binding to Ras, further increasing $\tau_{inactivation}$ (17). To determine if FRas-F expression increases the spread of Ras activation (Fig. S5) (22), we modulated FRas-F levels by changing the duration of expression and imaged Ras activation. FRas-F expression was quantified using post hoc immunofluorescence measurements (Fig. S6) (22). Ras activation spread along the dendrite even at the lowest FRas-F expression levels tested (~ 1.5 fold Ras over-expression, Fig. 2C-D). Furthermore, the spatial profile of Ras activity was similar across a wide range of FRas-F concentrations (Fig. 2C-D). FRas-F expression therefore did not distort the spatial spread of Ras activation.

We next investigated the mechanisms underlying the spread of Ras activity. Ras mobility could be a major determinant of the spread of Ras activity (Eq. 1). To measure mobility directly, we expressed H-Ras tagged with photoactivatable GFP (paGFP-Ras) (26) together with the cytoplasm marker mCherry. After photoactivation in single spines, the spine fluorescence decayed over seconds (τ = 4.17 ± 0.40 seconds), similar to membrane-targeted paGFP and

more than ten times slower than cytosolic paGFP (Fig. 3A-B) (3). These measurements suggest that Ras diffuses relatively freely within the plasma membrane. Constitutively active Ras (Ras G12V) diffused similarly to wild-type Ras (Fig. 3B) and had similar mobility with or without RBD expression (22); Ras activation and the binding of RBD to Ras therefore did not alter Ras diffusion appreciably. Near physiological temperatures (33° C), Ras mobility was enhanced by a factor of ~ 2, likely due to changes in membrane viscosity (Fig. 3B) (27). Within 30 seconds after photoactivation, more than 90% of the paGFP-Ras G12V fluorescence had decayed from the spine head (Fig. 3D). A similar fraction of membrane-targeted paGFP remained in the spine after 30 seconds (Fig. 3D). These studies imply that no major immobile fraction of active Ras exists in the spine. Ras over-expression could enhance diffusion by saturating Ras scaffolds (Fig. S5A) (22,28). However, the decay-time constant and the fraction of fluorescence remaining in the spine at 30 seconds were independent of paGFP-Ras G12V expression levels (Fig. 3C, E). These data argue that active endogenous Ras is highly mobile and does not associate strongly with immobile scaffolds in the spine.

The time constant of Ras inactivation could also modulate the spread of Ras activity (Eq. 1). Because the decay of Ras activity following uncaging stimuli includes both Ras inactivation and diffusion, we instead measured Ras inactivation following brief trains of back-propagating action potentials (bAPs), which activate Ras globally (Fig. 3F-G) (17). Since the length constant of Ras diffusion (~ 10 μm; Fig. 2B) is much longer than inter-spine distances, Ras molecules activated in both dendrites and spines sample the same population of GAPs independent of the stimulus. Following trains of bAPs, Ras activity decayed over minutes ($\tau_{inactivation}$ = 4.5 ± 0.4 minutes; Fig. 3G) (17). Near physiological temperatures (33° C), $\tau_{inactivation}$ was decreased by a factor of ~ 2 (Fig. 3H). Since this reduction in $\tau_{inactivation}$ was similar to the enhancement of Ras mobility (Fig. 3B), the spread of Ras activity is likely to be relatively independent of temperature (Eq. 1). The duration of Ras activity may be prolonged by FRas-F expression (Fig. S5B-C) (22). However, $\tau_{inactivation}$ was only weakly dependent on FRas-F expression levels (Fig. 3I). Extrapolation to the native case gave $\tau_{inactivation}$ ~ 2.9 minutes (Fig. 3I). Because RBD and exogenous Ras levels were correlated ($r = 0.89$, $P < 0.001$), the estimation of $\tau_{inactivation}$ takes into account the effects of both exogenous Ras and RBD expression. FRas-F therefore increased $\tau_{inactivation}$ by a factor of ~ 2 and thus the spatial spread by a factor of ~ 1.5 (Eq. 1). Active Ras in the native case is therefore expected to spread by diffusion over ~ 10 μm of dendrite, invading 10-20 synapses (22).

To address if diffusion of active Ras by itself can quantitatively explain the spread of Ras activity, we modeled the spread of Ras activation using a one-dimensional diffusion-reaction model. In the model, Ras is activated by stationary guanine nucleotide exchange factors (GEFs) in the stimulated spine and is inactivated by GAPs that are distributed homogeneously along the dendrite. By fitting our spatial Ras activity data (Fig. 2B) using a global regression analysis, we obtained estimates of the time constant of GEF activity, τ_{GEF} = 2.0 min, $\tau_{inactivation}$ = 4.5 minutes, and D = 0.65 $\mu m^2/s$. These estimates of $\tau_{inactivation}$ and D are identical to the values measured independently (Fig. 3) (22,29). We conclude that the spread of Ras activation can be explained by the rapid diffusion of active Ras.

What could be the function of the spread of Ras activation? Induction of LTP at a single synapse reduces the threshold for potentiation at neighboring synapses (16). Since the timescales (~ 5 minutes) and length scales (~ 10 μm) of Ras signaling and synaptic crosstalk (16) are identical, we tested if the spread of Ras activity is critical for the local modulation of the LTP induction threshold.

In a synaptic crosstalk experiment, LTP is induced at one spine (LTP spine) with a train of uncaging pulses; subsequently a subthreshold uncaging protocol, which by itself is too weak to trigger plasticity (Fig. S7C), is now sufficient to induce functional and structural plasticity

in a neighboring spine (sub spine) (16). If the spread of Ras activity is necessary for crosstalk, Ras-dependent signaling is likely required at a later time in the sub spine compared to the LTP spine. We induced LTP at a single spine and a short time (3 minutes) later locally applied a MEK inhibitor (20 μM U0126) to block Ras-ERK signaling; the inhibitor did not decrease the sustained spine volume change in the LTP spine appreciably (Fig. 4B-D). We then stimulated a neighboring spine with the subthreshold protocol. The MEK inhibitor substantially reduced the sustained spine enlargement in the sub spine (Fig. 4B-D), indicating that Ras-dependent signaling is necessary for crosstalk in plasticity.

Ras activity in the sub spine could be caused exclusively by the spread of Ras activity from the LTP spine, but may also include Ras directly activated in the sub spine by the subthreshold protocol. However, the subthreshold protocol alone did not induce detectable Ras activation (Fig. S7B). Similarly, in the crosstalk stimulus paradigm, the subthreshold protocol did not trigger additional Ras activation in the sub spine; the decay of Ras activation triggered by the LTP protocol was similar with and without application of the subthreshold protocol (compare Figs. 1G and 4E) (22). Furthermore, the magnitude of Ras activation in the sub spine prior to the subthreshold protocol, due to the spread of Ras activity, was correlated with the sustained spine enlargement in the sub spine (Fig. 4F). Together, these data indicate that the spread of Ras-dependent signaling is necessary for the local regulation of the LTP induction threshold.

We have shown that Ras signaling following LTP induction spreads along 10 μm of dendrite and invades neighboring spines. The timescale of Ras inactivation was on the order of minutes, compared with a spine-dendrite diffusional coupling time of seconds. Active Ras can therefore diffuse out of the spine head into the dendrite before inactivating. In contrast, Ca^{2+} is highly compartmentalized because it is extruded much more rapidly (tens of milliseconds) than the diffusional relaxation time between spine and dendrite (hundreds of milliseconds) (6). The diffusional barrier created by the narrow spine neck (2,3) may be important for rapid signals, such as Ca^{2+}, but is likely less significant for other diffusible signals with longer durations. Synapse-specific plasticity presumably is achieved by signaling molecules that are strongly tethered to postsynaptic scaffolds. The spread of Ca^{2+}-dependent signaling and local functional interactions at the level of plasticity (16) indicate that neighboring synapses are co-regulated. Synapses sharing a short stretch of dendrite may therefore form functional units within individual neurons (30).

Supplementary Material

Refer to Web version on PubMed Central for supplementary material.

References and Notes

1. Nimchinsky EA, Sabatini BL, Svoboda K. Annu. Rev. Physiol 2002;64:313. [PubMed: 11826272]
2. Svoboda K, Tank DW, Denk W. Science 1996;272:716. [PubMed: 8614831]
3. Bloodgood BL, Sabatini BL. Science 2005;310:866. [PubMed: 16272125]
4. Muller W, Connor JA. Nature 1991;354:73. [PubMed: 1682815]
5. Yuste R, Denk W. Nature 1995;375:682. [PubMed: 7791901]
6. Sabatini BL, Oertner TG, Svoboda K. Neuron 2002;33:439. [PubMed: 11832230]
7. Kennedy MB, Beale HC, Carlisle HJ, Washburn LR. Nat Rev Neurosci 2005;6:423. [PubMed: 15928715]
8. Kim MJ, Dunah AW, Wang YT, Sheng M. Neuron 2005;46:745. [PubMed: 15924861]
9. Tian X, et al. Embo J 2004;23:1567. [PubMed: 15029245]
10. Yun HY, Gonzalez-Zulueta M, Dawson VL, Dawson TM. Proc Natl Acad Sci U S A 1998;95:5773. [PubMed: 9576960]
11. Zhu JJ, Qin Y, Zhao M, Van Aelst L, Malinow R. Cell 2002;110:443. [PubMed: 12202034]

12. Malenka RC, Bear MF. Neuron 2004;44:5. [PubMed: 15450156]
13. Matsuzaki M, Honkura N, Ellis-Davies GC, Kasai H. Nature 2004;429:761. [PubMed: 15190253]
14. Tsuriel S, et al. PLoS Biol 2006;4:e271. [PubMed: 16903782]
15. Gray NW, Weimer RM, Bureau I, Svoboda K. PLoS Biol 2006;4
16. Harvey CD, Svoboda K. Nature 2007;450:1195. [PubMed: 18097401]
17. Yasuda R, et al. Nat Neurosci 2006;9:283. [PubMed: 16429133]
18. Mochizuki N, et al. Nature 2001;411:1065. [PubMed: 11429608]
19. Rocks O, et al. Science 2005;307(5716):1746. [PubMed: 15705808]
20. Piston, DW.; Sandison, DR.; Webb, WW. Time-Resolved Laser Spectroscopy in Biochemistry III. Lakowicz, JR., editor. SPIE; Bellingham, WA: 1992. p. 379-389.
21. Gratton E, Breusegem S, Sutin J, Ruan Q, Barry N. J Biomed Opt 2003;8:381. [PubMed: 12880343]
22. See Supporting Online Materials available on Science Online.
23. Nimchinsky EA, Yasuda R, Oertner TG, Svoboda K. J Neurosci 2004;24:2054. [PubMed: 14985448]
24. Kopec CD, Li B, Wei W, Boehm J, Malinow R. J Neurosci 2006;26:2000. [PubMed: 16481433]
25. Fivaz M, Bandara S, Inoue T, Meyer T. Curr Biol 2008;18:44. [PubMed: 18158244]
26. Patterson GH, Lippincott-Schwartz J. Science 2002;297:1873. [PubMed: 12228718]
27. Reits EA, Neefjes JJ. Nat Cell Biol 2001;3:E145. [PubMed: 11389456]
28. Niv H, Gutman O, Kloog Y, Henis YI. J Cell Biol 2002;157:865. [PubMed: 12021258]
29. Lommerse PH, et al. Biophys J 2004;86:609. [PubMed: 14695305]
30. Losonczy A, Makara JK, Magee JC. Nature 2008;452:436. [PubMed: 18368112]
31. We thank Nima Ghitani, Barry Burbach, Catherine Zhang, Brenda Shields, and Helen White for technical assistance, Noah Gray for help with immunostaining, Linda van Aelst for helpful discussions, and Josh Dudman for comments on the manuscript. This work was supported by HHMI, NIH, NYSTAR, a David and Fanny Luke Fellowship (C.D.H.), Burroughs Wellcome Fund (R.Y.), Dana Foundation (R.Y.), NAAR (R.Y.), NIH/NIMH (R.Y.), and NARSAD (H.Z.).

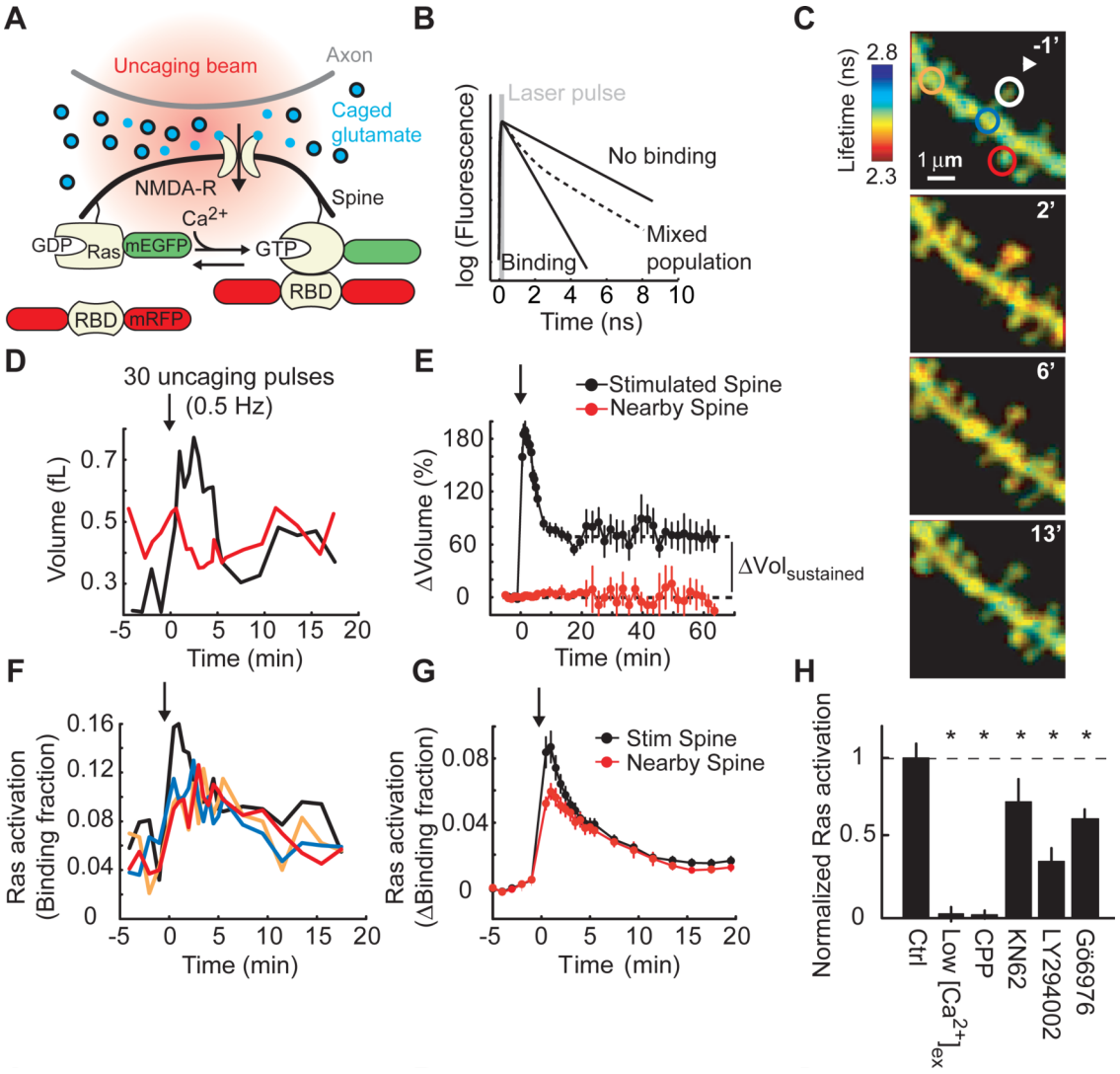

Figure 1. Ras activation in individual dendritic spines during plasticity induction

(A) Experimental geometry.

(B) Schematic of fluorescence decay curves following pulsed excitation. Slow and fast components correspond to free donor and donor bound to acceptor, respectively. FRET decreases fluorescence lifetime.

(C) FLIM images of Ras activity. At time = 0, 30 uncaging pulses (0.5 Hz) were applied to the spine marked by the arrowhead in low (nominally 0 mM) extracellular Mg^{2+}. Warmer colors indicate shorter lifetimes and higher levels of Ras activation.

(D) Changes in spine volume. Colors correspond to the circles in (C). Arrow, time of stimulus.

(E) Spine volumes for the stimulated and nearby (< 4 μm) spines (−5 to 20 minutes: 91 spines; > 20 minutes: 9 spines, mean ± sem). $\Delta Vol_{sustained}$ is the volume difference between 15.5-19.5 minutes and the baseline volume.

(F) Ras activation. Colors correspond to the circles in (C).

(G) Ras activation in the stimulated and nearby spines (82 spines, mean ± sem).

(H) Pathways to Ras activation. Ras activation was the average binding fraction at 1-3 minutes minus baseline, normalized to the control condition. Numbers of spines: 82 Ctrl, 11 Low $[Ca^{2+}]_{ex}$ (200 μM), 12 CPP (10 μM), 27 KN62 (10 μM), 20 LY294002 (20 μM), and 23 Gö6976 (1 μM). Error bars indicate mean ± sem. Asterisks indicate $P < 0.05$ versus control.

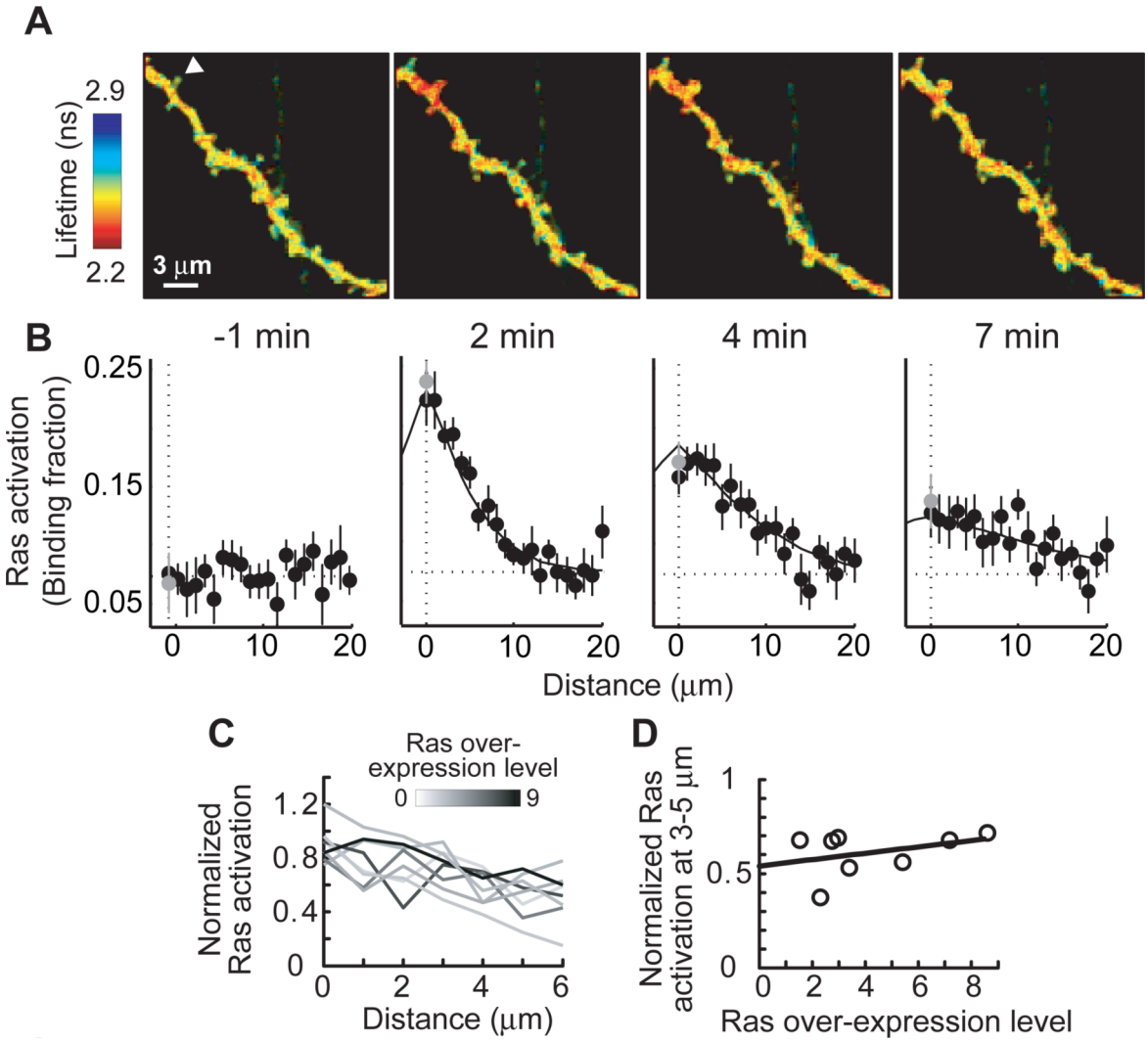

Figure 2. Spatial spread of Ras activity

(A) Fluorescence lifetime images of Ras activity. At time = 0 LTP was induced at the spine marked by an arrowhead.

(B) The spatial spread of Ras activation at different time points. Black circles indicate distances along the dendrite relative to the stimulated spine (gray circle; $n = 11$, mean ± sem). The solid line shows the fitted profile of Ras activation derived from a 1-D diffusion-reaction model (22).

(C) The spatial spread of Ras activation (Ras activation, normalized to peak Ras activation in the stimulated spine, two minutes post-stimulus) at various expression levels.

(D) Normalized Ras activation 3-5 μm from the stimulated spine. $r = 0.36$, $P > 0.3$, $n = 8$.

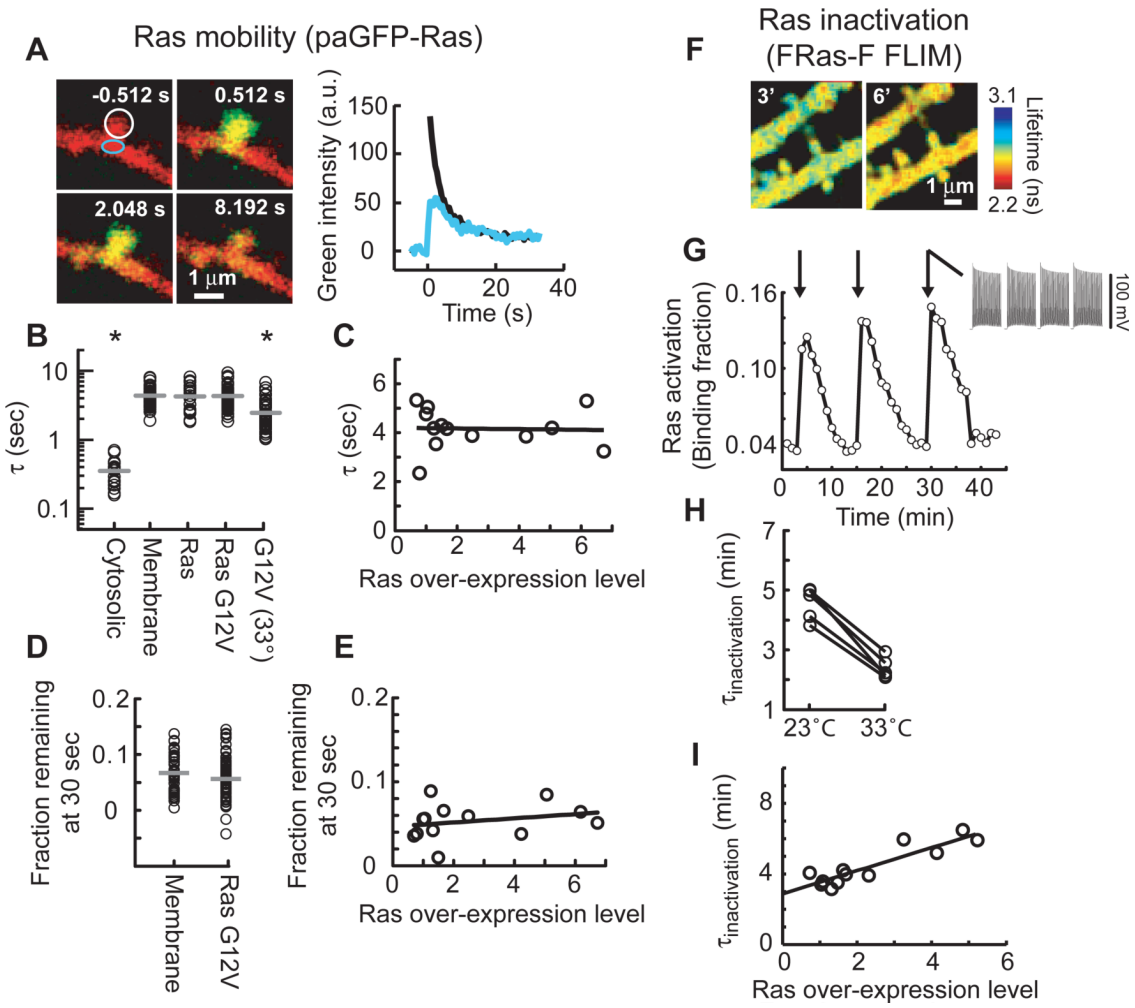

Figure 3. Ras mobility and the time constant of Ras inactivation

(A) Left: Spine before and after photoactivation (green, paGFP-Ras; red, mCherry). Right: Time course of activated paGFP-Ras in the spine (black) and parent dendrite (blue).

(B) Decay time constants of paGFP fluorescence in the photoactivated spine. Horizontal bars, mean. Numbers of spines: 17 cytosolic, 46 membrane, 21 Ras, 84 Ras G12V, 52 Ras G12V (33° C). Asterisks indicate $P < 0.05$ versus paGFP-Ras G12V (23° C).

(C) Decay time constants of paGFP-Ras G12V fluorescence at varying expression levels. $r = -0.05$, $P > 0.8$, $n = 13$.

(D) Fraction of paGFP fluorescence remaining in the spine 30 seconds after photoactivation. Horizontal bars, mean. Number of spines: 46 membrane, 84 Ras G12V. $P > 0.7$.

(E) Fraction of paGFP-Ras G12V fluorescence remaining in the spine at 30 seconds at varying expression levels. $r = 0.25$, $P > 0.4$, $n = 13$.

(F) Fluorescence lifetime images before and after trains of back-propagating action potentials (40 APs at 83 Hz, repeated 4 times every 5 seconds).

(G) Time course of Ras activation for the experiment shown in (F). Arrows, action potential stimuli.

(H) $\tau_{inactivation}$ at 23° C and 33° C. Ras inactivation was measured at both temperatures in individual cells. $n = 5$, $P < 0.001$.

(I) Ras inactivation at varying expression levels. $r = 0.8$, $P < 0.01$, slope = 0.6 minutes per fold over-expression, intercept = 2.9 minutes. $n = 12$.

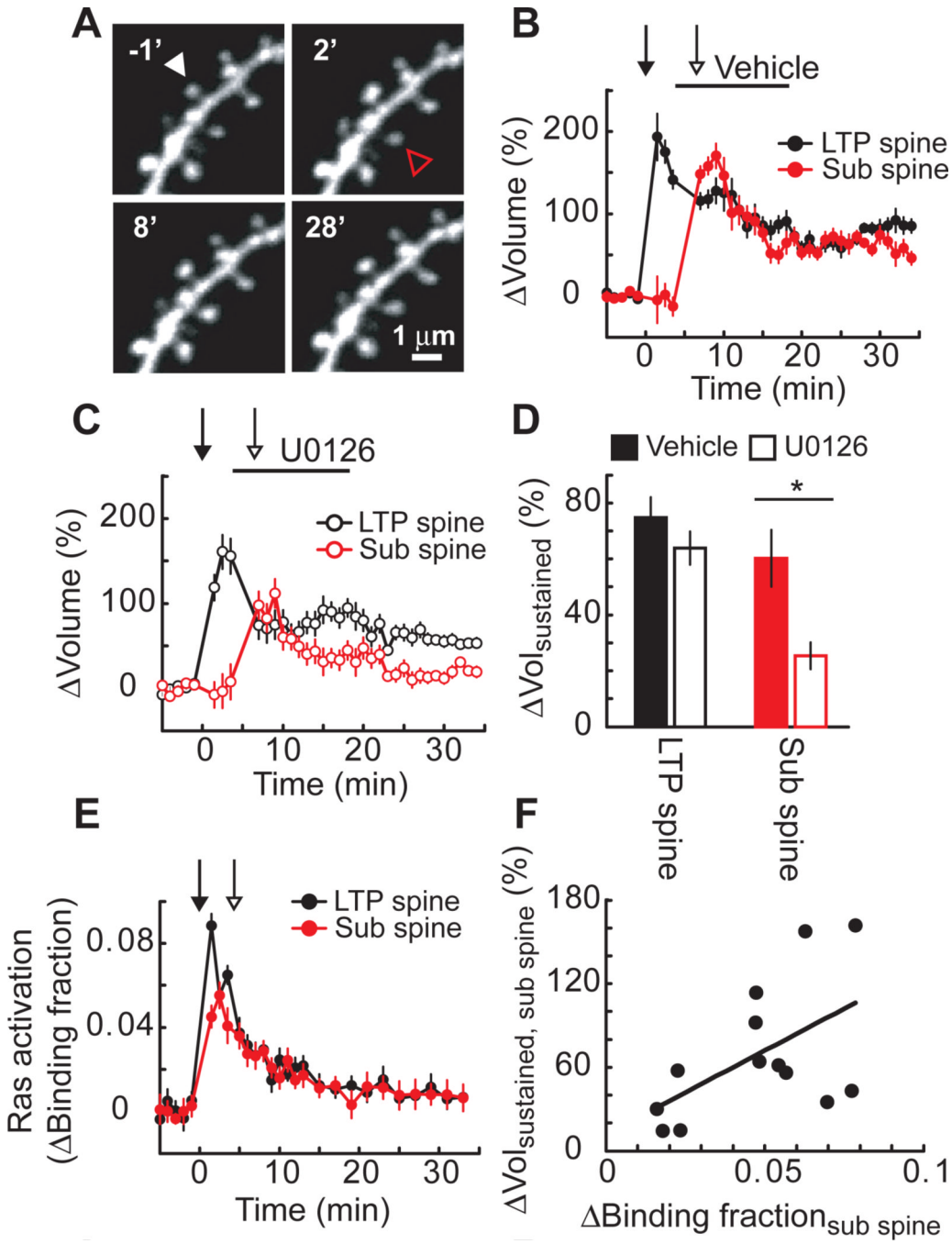

Figure 4. Spread of Ras signaling and synaptic crosstalk

(A) Time-lapse images of a GFP-expressing pyramidal neuron in an acute hippocampal brain slice. At time = 0, 30 uncaging pulses (0.5 Hz, 4 ms pulse duration, LTP protocol) were applied to the spine marked by a white arrowhead (LTP spine) in low extracellular Mg^{2+}. At time = 3 minutes, vehicle (0.1% DMSO) was pressure applied locally from a glass pipette until time = 17 minutes. At time = 5.5 minutes, the subthreshold protocol (30 uncaging pulses, 0.5 Hz, 1 ms pulse duration) was applied to a nearby spine (sub spine, red arrowhead).

(B) Spine volume changes in the vehicle condition (11 spines, mean ± sem).

(C) Spine volume changes in the 20 μM U0126 condition (11 spines, mean ± sem).

(D) Sustained changes in spine volume. Error bars indicate mean ± sem. Asterisk indicates $P < 0.05$.

(E) Ras activation in the LTP and sub spines during the crosstalk paradigm in cultured hippocampal slices. At time = 0, the LTP protocol was applied to the LTP spine, and 3.5 minutes later the subthreshold protocol was applied to the sub spine (13 spines, mean ± sem).

(F) Relationship between Ras activation and the sustained spine enlargement in the sub spine during crosstalk. ΔBinding fraction was measured before the subthreshold protocol (1.5 to 3.5 minutes after the LTP protocol). $r = 0.54$, $P = 0.05$.